N91-10302

TEST/SEMI-EMPIRICAL ANALYSIS OF A CARBON/EPOXY FABRIC STIFFENED PANEL

E.E. Spier and J.A. Anderson
Rohr Industries, Inc.
San Diego, California

Test/Semi-Empirical Analysis

Since 1975, extensive testing of carbon/epoxy tape plates and stiffened panels has been performed (Reference 1 through 6). Attempts were made to predict the crippling failure of stiffened panels, fabricated from C/Ep tape, using the non-linear option in the STAGS computer code (Reference 7). However, no meaningful results were acquired. Therefore, a semi-empirical crippling method was developed.

To date, a semi-empirical analysis method has not been developed for plates and stiffened panels manufactured from C/Ep fabric. The purpose of this work-in-progress is to present a semi-empirical analysis method developed to predict the buckling and crippling loads of carbon/epoxy fabric blade stiffened panels in compression. This is a hand analysis method comprised of well known, accepted techniques, logical engineering judgements, and experimental data that results in conservative solutions. In order to verify this method, a stiffened panel was fabricated and tested. Both the test and analysis results are presented.

Buckling/Crippling Test Specimen

This figure shows the test panel configuration. It consists of a skin with three blade stiffeners. The blade stiffeners contain flanges which were cocured to the skin. The entire panel was made from Hercules AS4/3501-5A carbon/epoxy fabric except for the C/Ep tow used at the flange/blade intersection. This C/Ep tow provides structural integrity at the joint, including significant torsional stiffness provided at the blades.

The blade stiffened panel was completely A and C-scanned and no defects were found. Prior to test, the panel was machined and assembled with potted aluminum end channels. The end surfaces were then ground parallel within .001 inch.

The unloaded edges of the outer skin elements were supported by split rigid steel tubes to simulate simple support boundary conditions. This isolates the three stiffeners as though they were in a much wider stiffened panel. Thus, it was sufficient to analyze just the middle stiffener and apply this result to all three. The load carried by the skin adjacent to each split tube was justifiably neglected because it is such a small percentage of the total panel load.

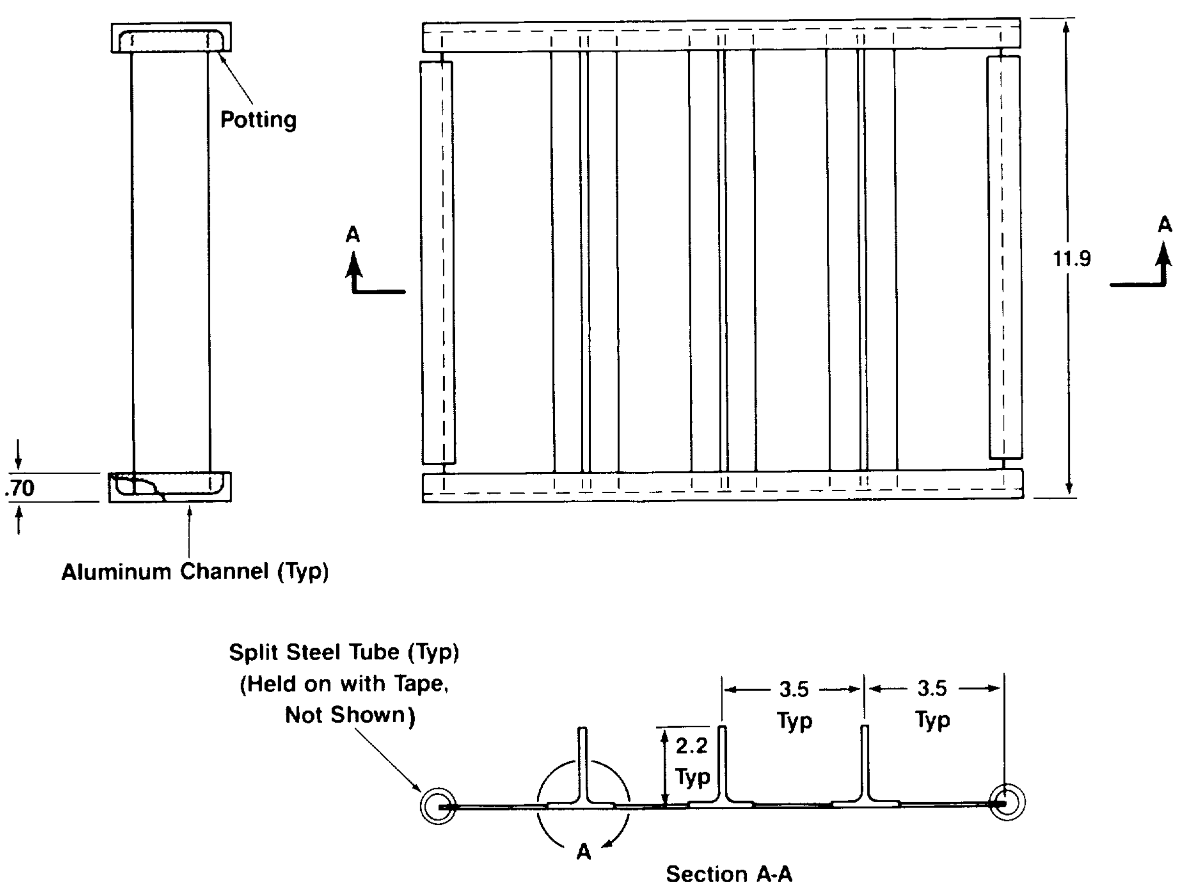

Detail A - Cross Section

This is the cross section of the stiffener/skin intersection. As mentioned above, the region adjacent to the blade, between the flange & skin, was filled with longitudinal carbon/epoxy tow. This juncture provides substantial support to the skin and the blades. However, the load carrying capability of the tow is neglected in the analysis.

The panel elements were configured so that the skin buckled first and the blades buckled second. Thus, the flanges, which buckle last, support both the skin and the blades.

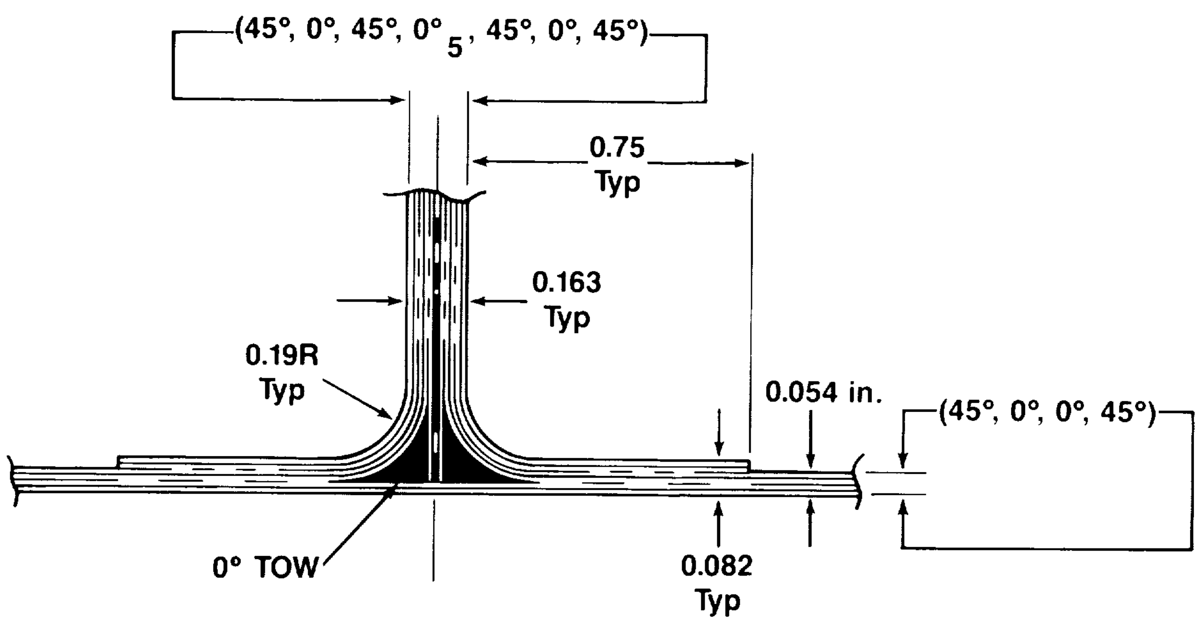

Typical Blade/Skin Intersection

This is a photomicrograph of the manufactured stiffener/skin intersection. Good consolidation was achieved and structural integrity of this joint was expected. The curvature of the blade middle plies was inadvertent, but no reduction of boundary constraint was predicted.

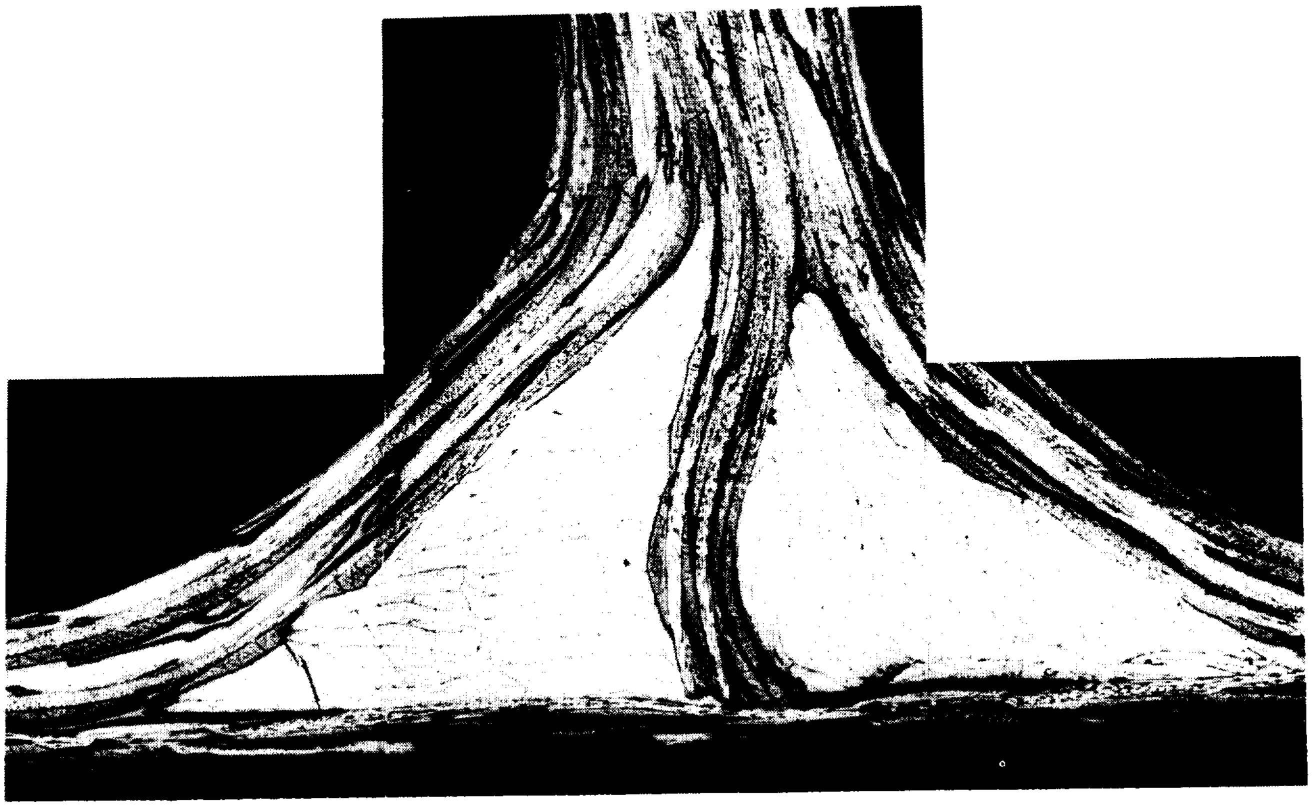

No-Edge-Free Postbuckling Test

In order to develop a semi-empirical stability analysis for carbon/epoxy fabric stiffened panels, empirical buckling and crippling curves for plates were generated. The plates tested were symmetric and balanced C/Ep fabric laminates. Each test plate was rectangular with clamped boundary conditions on the loaded edges (i.e., the short sides). Various b/t ratios were examined.

Two unloaded edge boundary conditions were tested. The first, designated "no-edge-free", was simply supported on both unloaded edges. The second, designated "one-edge-free", was simply supported on one edge and free on the other.

This is a typical no-edge-free plate test in compression. The unloaded edges are supported by steel v-blocks, simulating simple-support boundary conditions. The test specimen is in a postbuckled state. A full longitudinal wave can be seen.

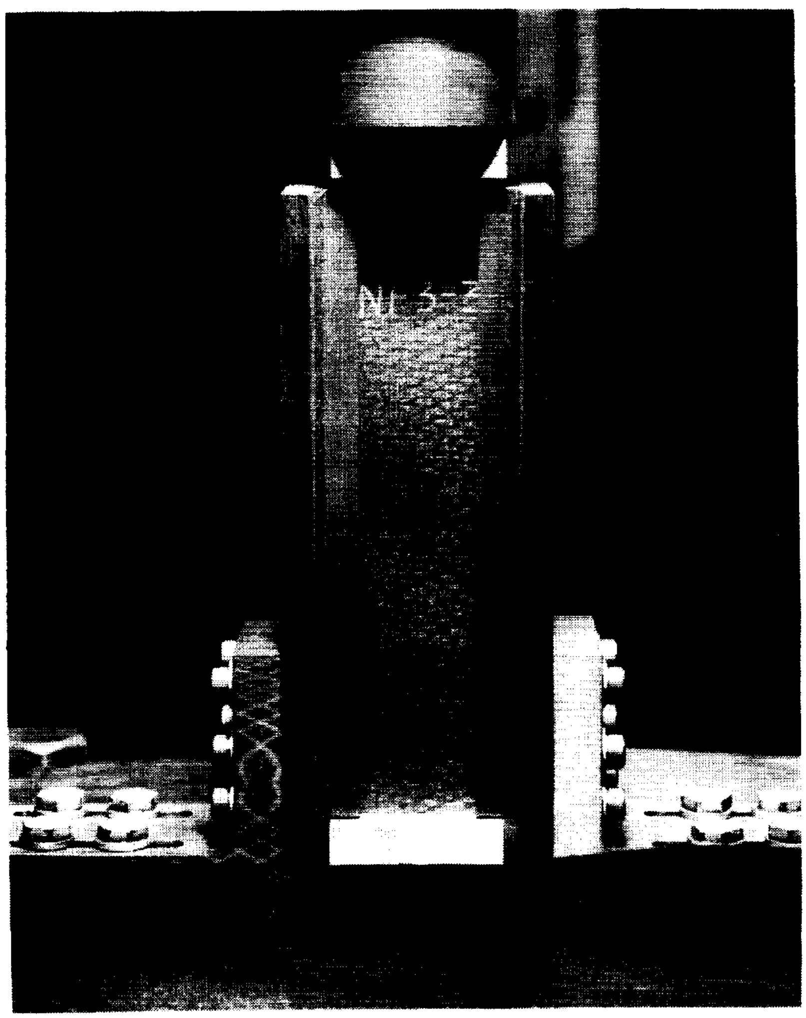

No-Edge-Free Crippling Test

Postbuckling failure of the no-edge-free compression test specimen is shown. This failure is referred to as "crippling". The type of failure shown is typical for carbon/epoxy fabric plates.

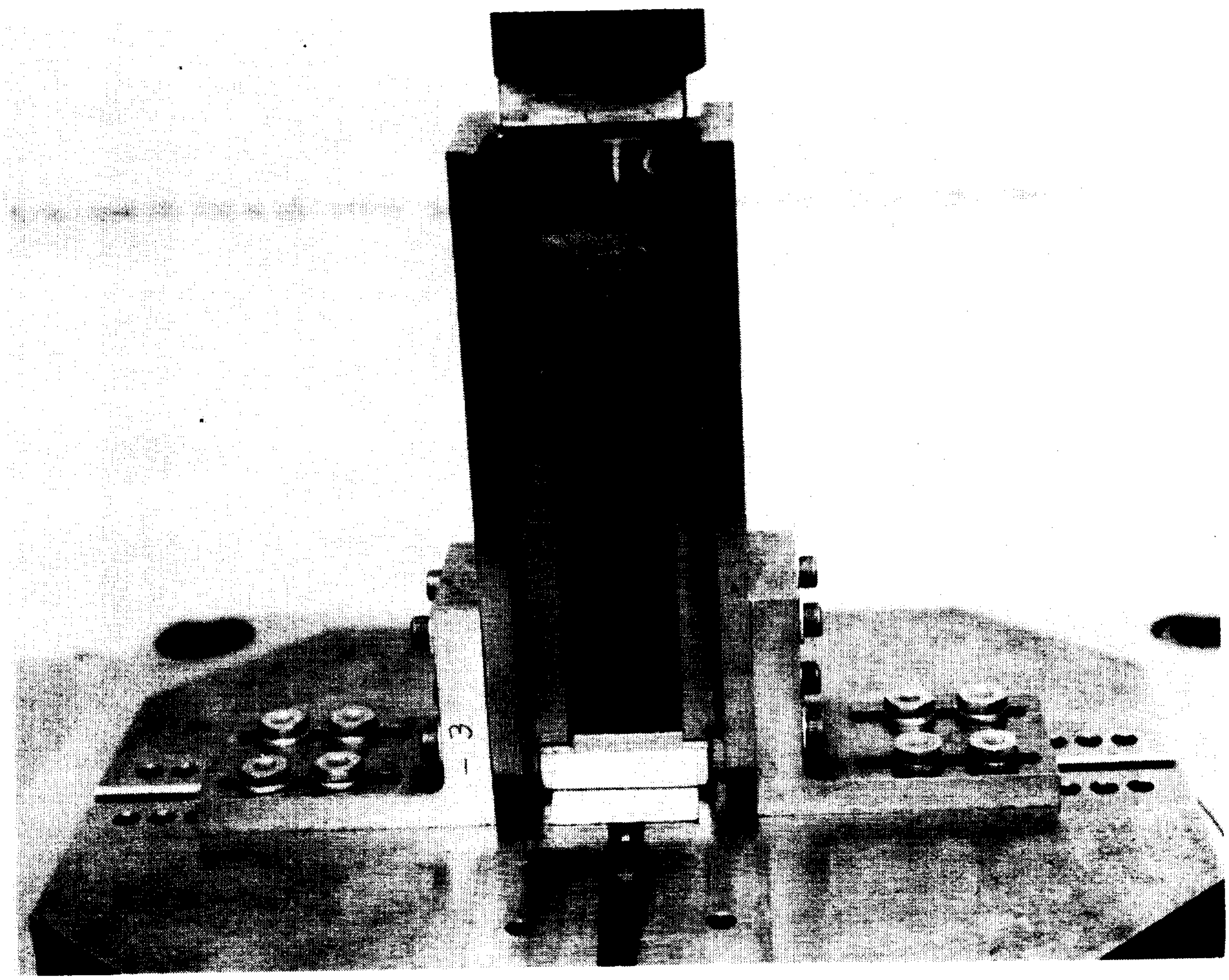

ORIGINAL PAGE
BLACK AND WHITE PHOTOGRAPH

One-Edge-Free Postbuckling Test

This is a typical one-edge-free plate test in compression. One unloaded edge is supported by a steel v-block, simulating a simple-support boundary condition while the other unloaded edge is free. The test specimen is in a postbuckled state. One longitudinal half-wave can be seen.

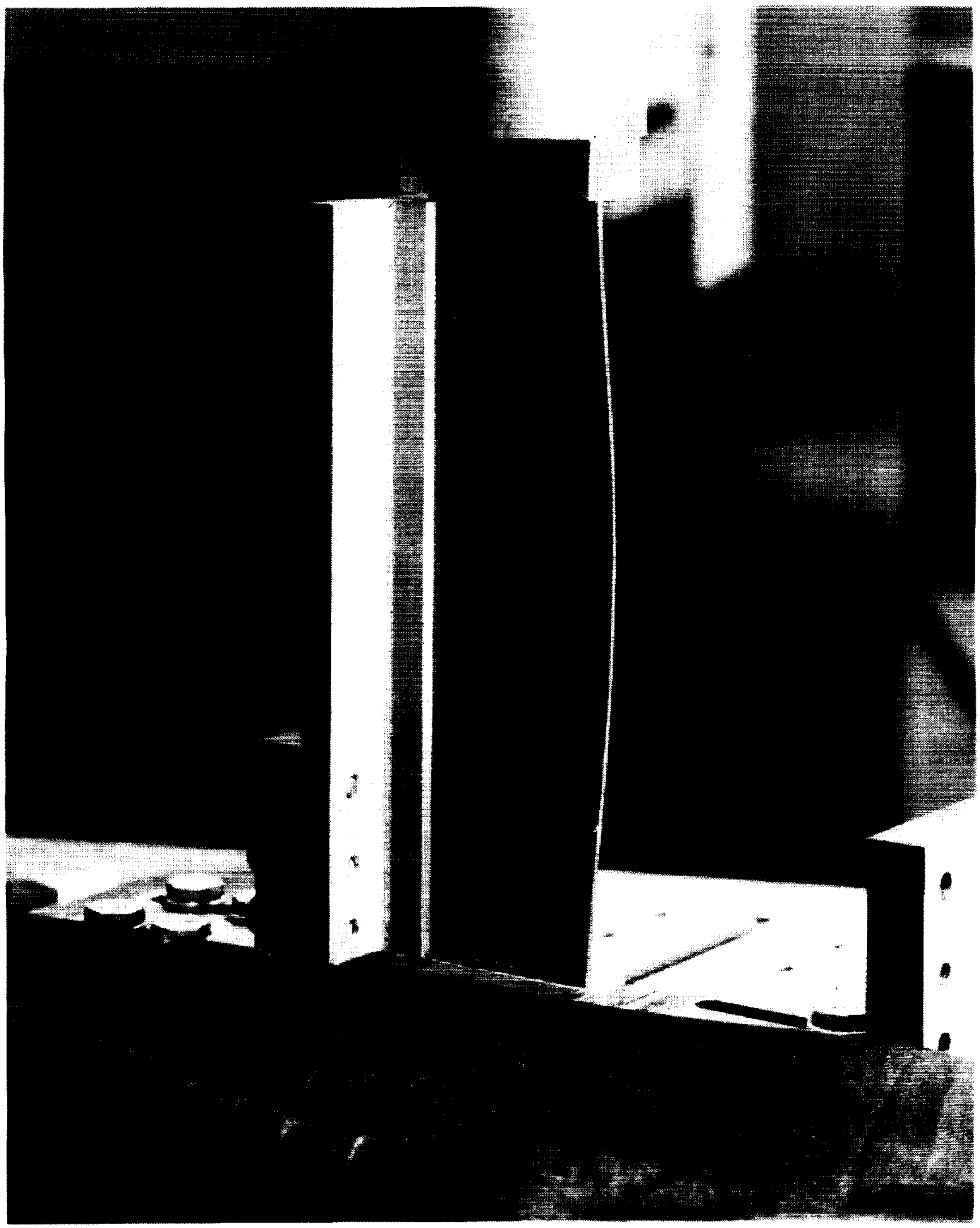

ORIGINAL PAGE
BLACK AND WHITE PHOTOGRAPH

One-Edge-Free Crippling Test

Postbuckling failure (or crippling) of the one-edge-free compression test specimen is shown. This type of failure is typical for carbon/epoxy fabric plates.

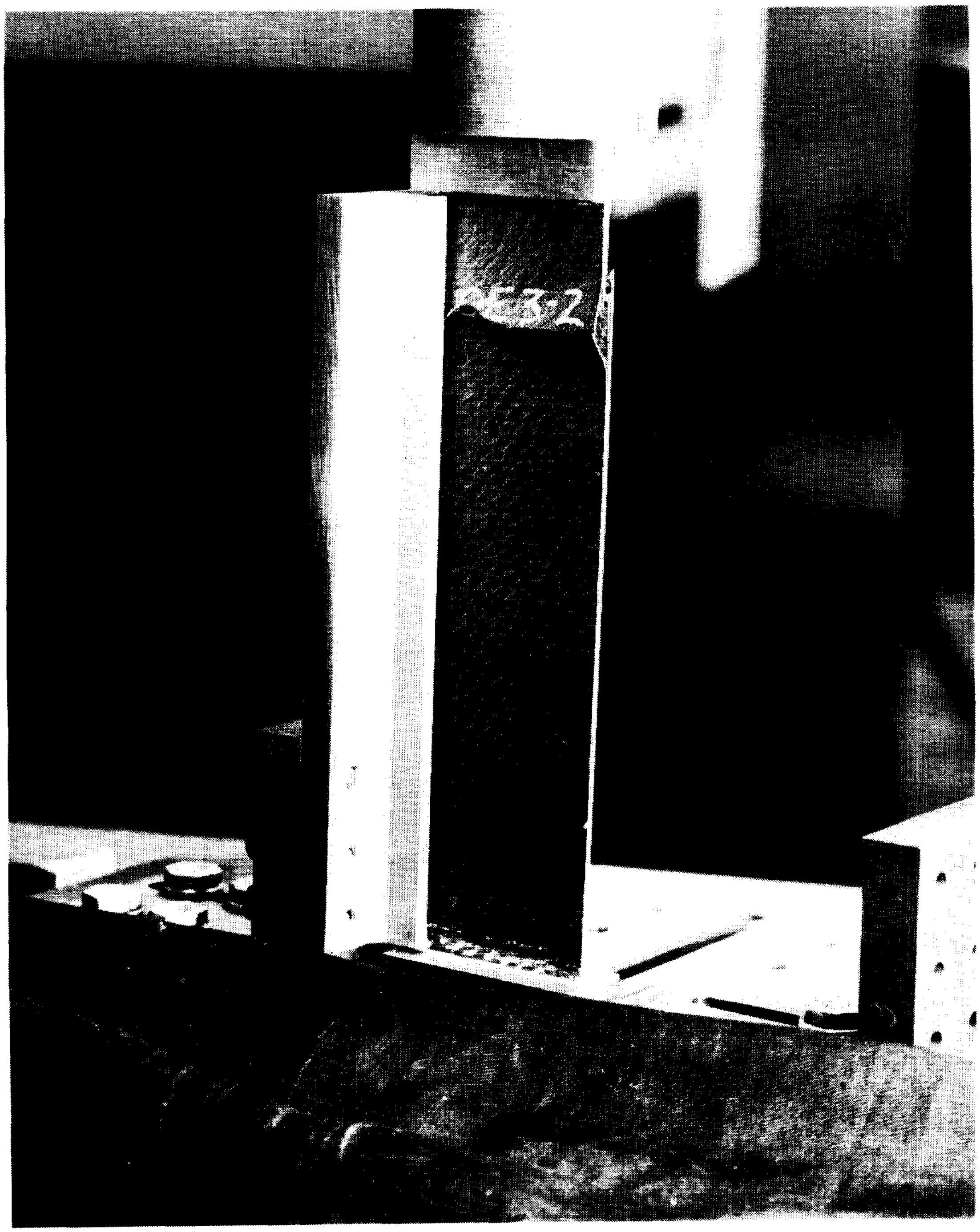

Typical load-Displacement Curve from Crippling Test

This is a typical load-displacement curve for a plate compression test, either no-edge-free or one-edge-free. Displacement refers to the end-shortening of the test specimen. Buckling (P^{cr}) occurs at the bifurcation point of the linear curve. Crippling (P^{cc}) is the maximum postbuckling load that is reached prior to failure.

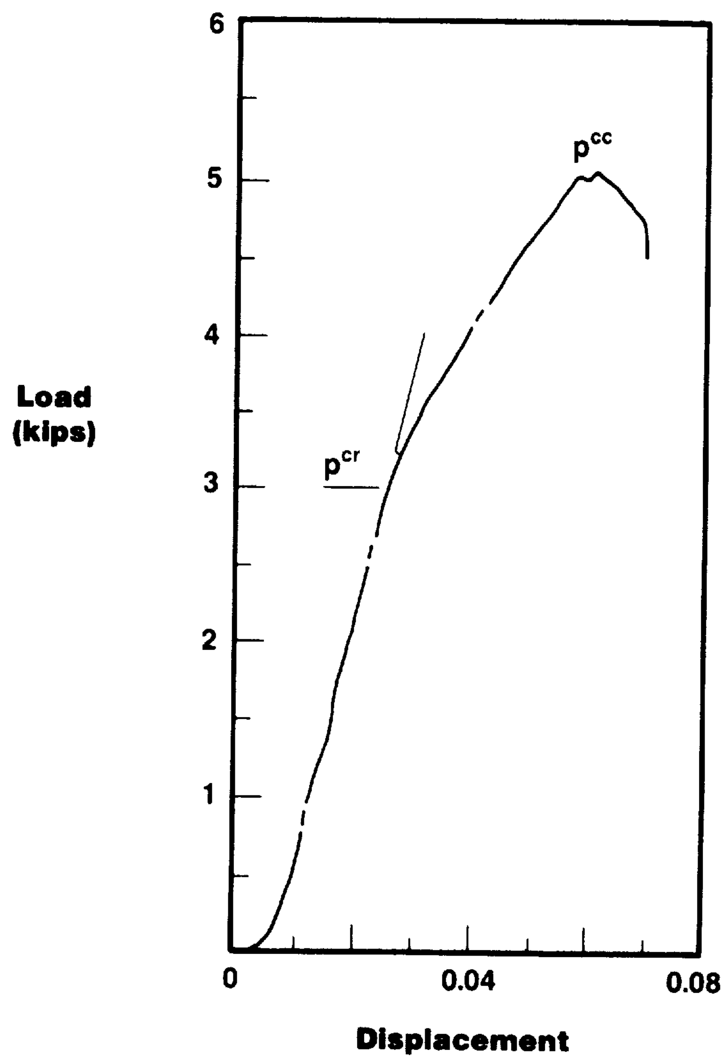

No-Edge-Free Buckling Graph

The no-edge-free buckling test data shown defines an empirical buckling curve for composites with similar layups. The ordinate is the ratio of the test buckling stress divided by the calculated classical buckling stress (F^{cr}/F^{cr}_{cl}). The abscissa is the width-to-thickness (b/t) ratio. The value for the classical buckling strength (F^{cr}_{cl}) can be obtained by using one of the following equations.

* Simply Supported Unloaded Edges

$$F^{cr,u,\phi E}_{cl,i,ss} = \frac{2\pi^2}{tb^2}\left[(D_{11}D_{22})^{\frac{1}{2}} + D_{12} + 2D_{66}\right]$$

* Fixed Unloaded Edges

$$F^{cr,u,\phi E}_{cl,i,fx} = \frac{\pi^2}{tb^2}\left[4.6(D_{11}D_{22}) + 2.67(D_{12}) + 5.33(D_{66})\right]$$

The classical buckling stress can be quite unconservative at low b/t ratios. However, the classical theory is accurate at b/t ratios greater than 50.

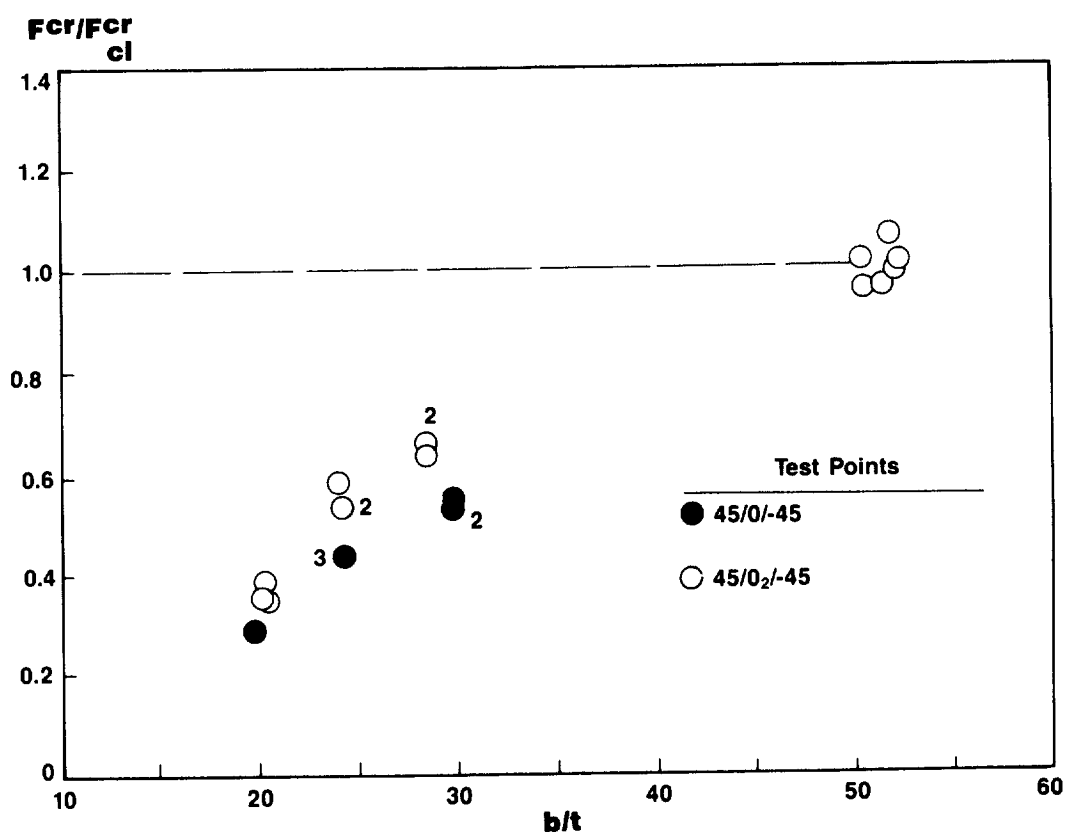

One-Edge-Free Buckling Graph

The one-edge-free buckling test data shown defines an empirical buckling curve for similar composite layups. The value for the one-edge-free classical buckling strength can be obtained by using the following equation.

$$F_{cl,i,ss}^{cr,u,1E} = \frac{12D_{66}}{tb^2} + \frac{\pi^2 D_{11}}{t(L')^2} \quad \text{where } L' = \frac{L}{(\sqrt{C})}$$

C is the end-fixity coefficient of columns and is approximately equal to 3.6 for potted end columns in a test machine.

This graph and its use is similar to that for no-edge-free composite plates. The discrepancy between classical and experimental buckling at low b/t ratios is the result of low transverse shear stiffness (Reference 8). This effect is insignificant at large b/t ratios.

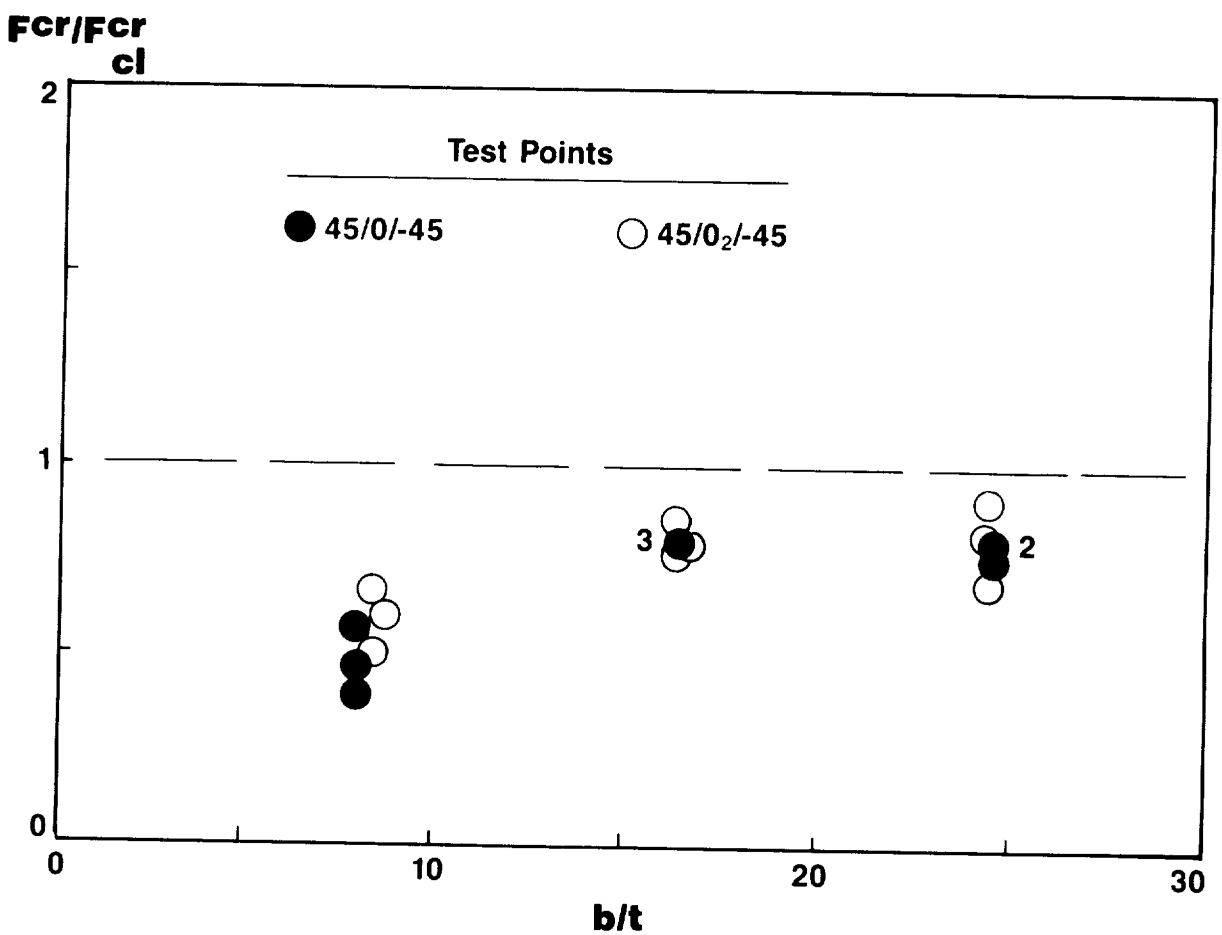

Laminate Ultimate Compressive Strength

This figure shows the ultimate compressive strength (F^{cu}) for AS4/3501-5A fabric 0°, 45° composite laminates. This data was generated because F^{cu} is required for the nondimensional empirical crippling curves which follow.

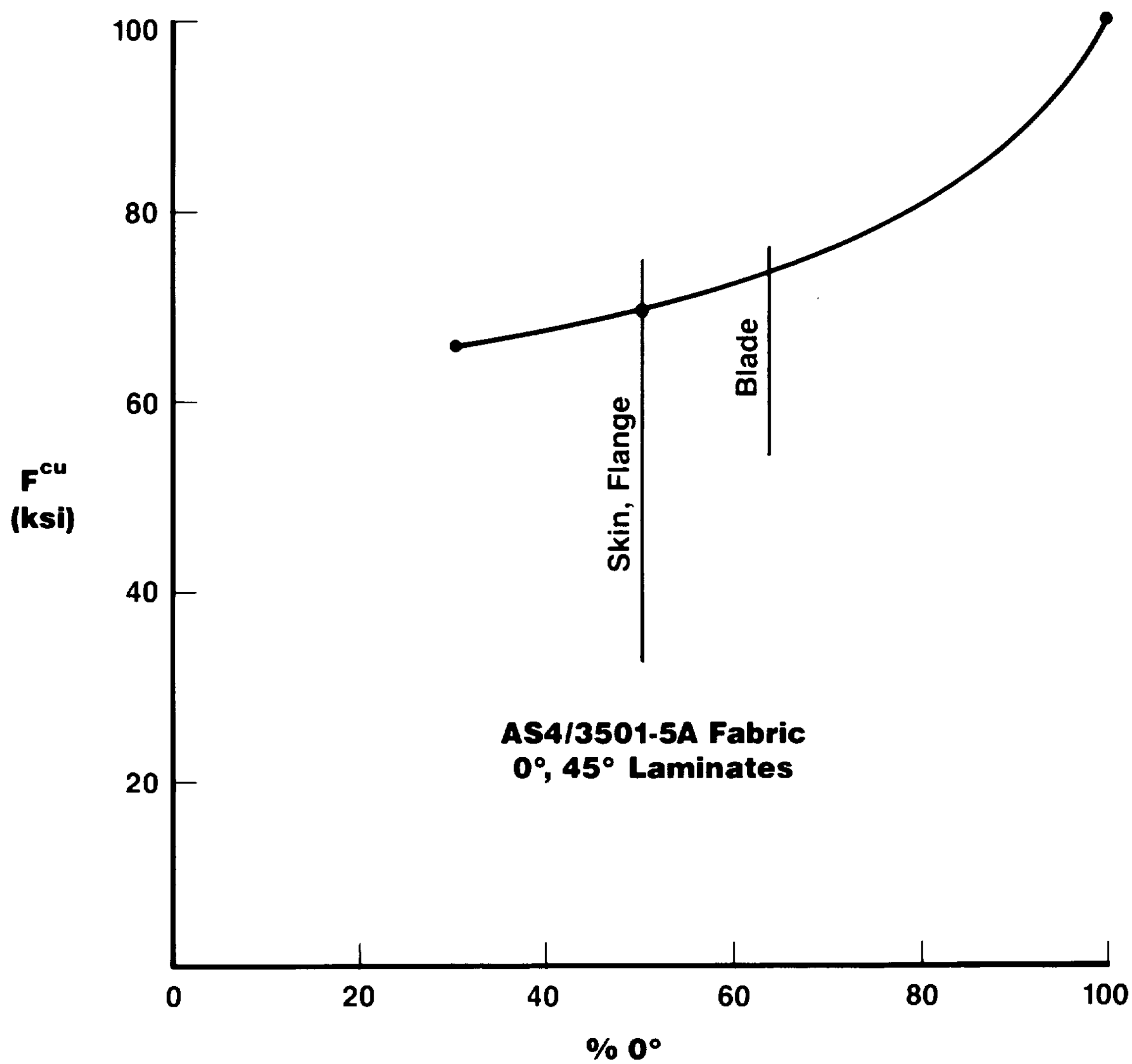

No-Edge-Free Crippling Graph

The no-edge-crippling test data shown was used to define the approximate mean crippling graph. The ordinate is the crippling stress (F^{cc}) divided by the classical buckling stress (F^{cr}_{cl}), while the abscissa is the ultimate compressive stress (F^{cu}) divided by F^{cr}_{cl}. Thus, for plates with similar layups, where the value for F^{cu} is known and F^{cr}_{cl} can be calculated, the predicted crippling stress may be obtained.

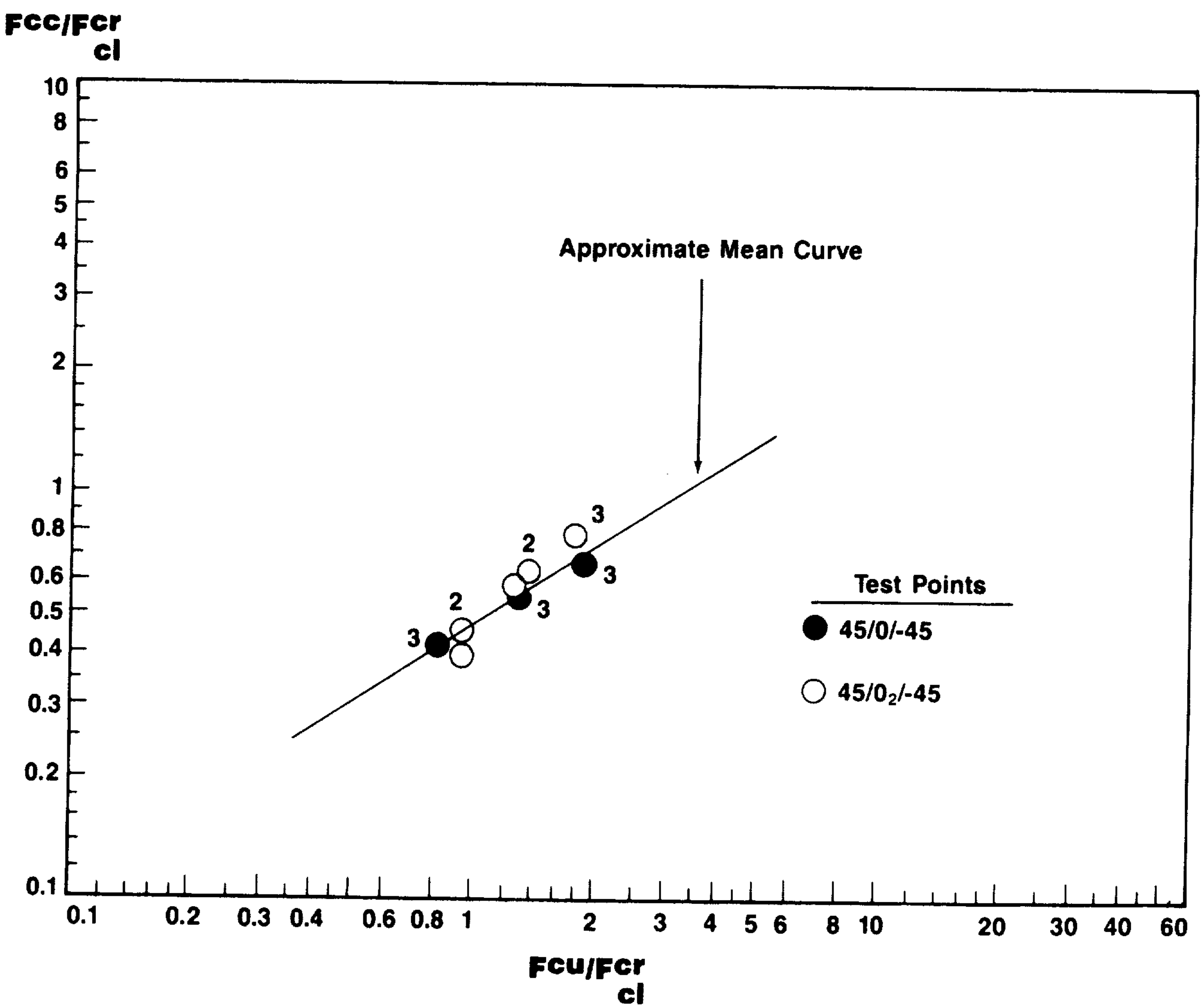

One-Edge-Free Crippling Graph

The one-edge-crippling graph shown is defined and utilized in a similar fashion to that for the no-edge-free graph.

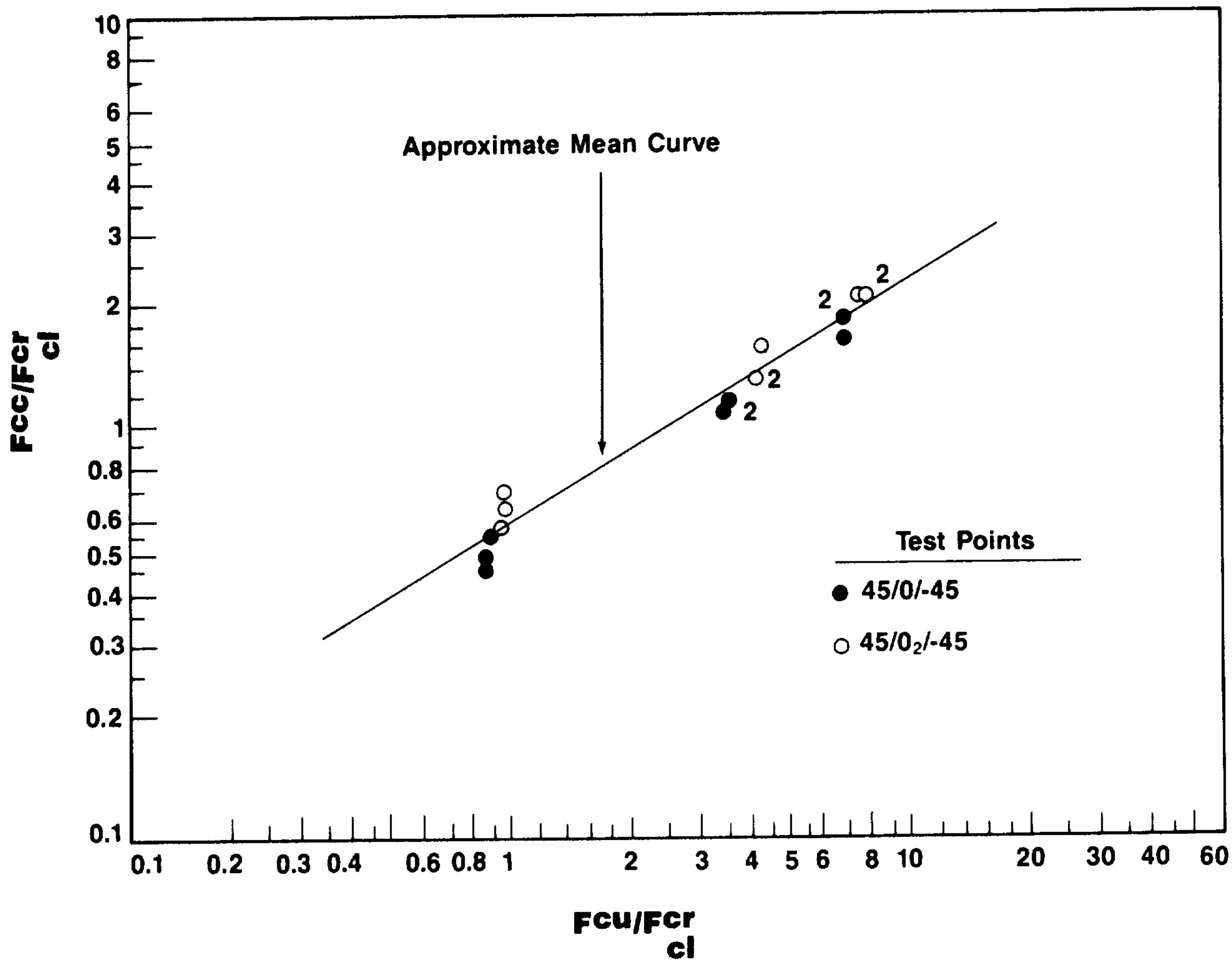

Crippling Strength Predictions

Armed with the empirical buckling and crippling curves, a step by step process can be used to calculate the crippling strength of the middle stiffener's blade and flanges. The classical buckling strains ($\epsilon_{*}^{cr,st}$) for the blade and flange elements are .00309 in/in and .00582 in/in, respectively. In this case, the blade buckles first and causes the flange element to buckle prematurely. Therefore, the minimum classical buckling strain is equal to .00309 in/in.

The classical buckling strain is theoretical, not actual, and is referred to as a pseudo-strain. Using this strain (.00309 in/in) and the elastic modulus ($E_{Th,i}^{c,u}$), the pseudo-buckling stresses ($F_{*,i}^{cr,u}$) are calculated. The compression strengths ($F_{n,u}^{cu,i}$) are found from lamination theory or test results. The resulting pseudo-crippling stresses ($F_{*,i}^{cc,u}$) are then obtained from the one-edge-free empirical crippling curve.

However, the empirical crippling curve was developed from testing plates with simply supported boundary conditions. The actual blade has a boundary condition better than simply supported but certainly not fixed. Consequently, the boundary condition was assumed to be equal to one-half the increase in fixity from simply supported to fully fixed. This correction factor (Ca) is only applied to the blade because the flange supports the blade until it buckles, but at that point, the blade cannot provide greater than simple-support to the flange. The crippling load of the middle stiffener is obtained by summing the stiffener element pseudo-crippling loads ($C_a P_{*,i}^{cc,b} + 2P_{*,i}^{cc,f}$).

1	2	3	4	5	6	7	8	9	10	11	12
ELEMENT	A_i^u (in.^{2})	$E_{Th,i}^{c,u}$ (psi)	$\epsilon_{*}^{cr,st}$	$F_{*,i}^{cr,u} = 3 \cdot 4$ (psi)	$F_{n,i}^{cu,u}$ (psi)	$F_{n,i}^{cu,u}/F_{*,i}^{cr,u} = 6 / 5$	$F^{cc}/F_{*,i}^{cr,u}$	$F_{*,i}^{cc,u} = 5 \cdot 8$ (psi)	$P_{*,i}^{cc,u} = 2.9$	C_a	$C_a P_{*,i}^{cc,u} = 10 \cdot 11$ (lb)
BLADE	0.326	7.60×10^6	0.00309	23,457	73,000	3.11	1.19	29,913	9,100	1.5	13,650
FLANGE	0.062	7.47×10^6	0.00309	23,082	69,000	2.99	1.18	27,237	1,689	1.0	1,689

Effective-Width from Compressive Stress Distribution in a Buckled Flat Plate

In order to calculate the crippling strength of the panel, the skin, which buckles first, must also be considered. This requires an effective-width concept which was originally developed for metal structures by T. von Karman (Reference 9). In this method, a uniform compressive stress ($\sigma^{c,es}_{,i}$), at the same average strain as the stiffener at crippling, acts on a width of plate w^{es}_i directly adjacent to the supported edges. The value of w^{es}_i is adjusted so the $(\sigma^{c,es}_{,i})*(\hat{w}^{es}_i)*(t^{sk}_i)$ is equal to the total load carried by the skin on one side of the stiffener. Thus, for a skin having the postbuckled distribution shown, the effective-width can be found using von Karman's equation. The value of $(\sigma^{c,es}_{,i})$ depends upon the magnitude of the applied design load or, in the case of analyzing a tested panel, the failure load.

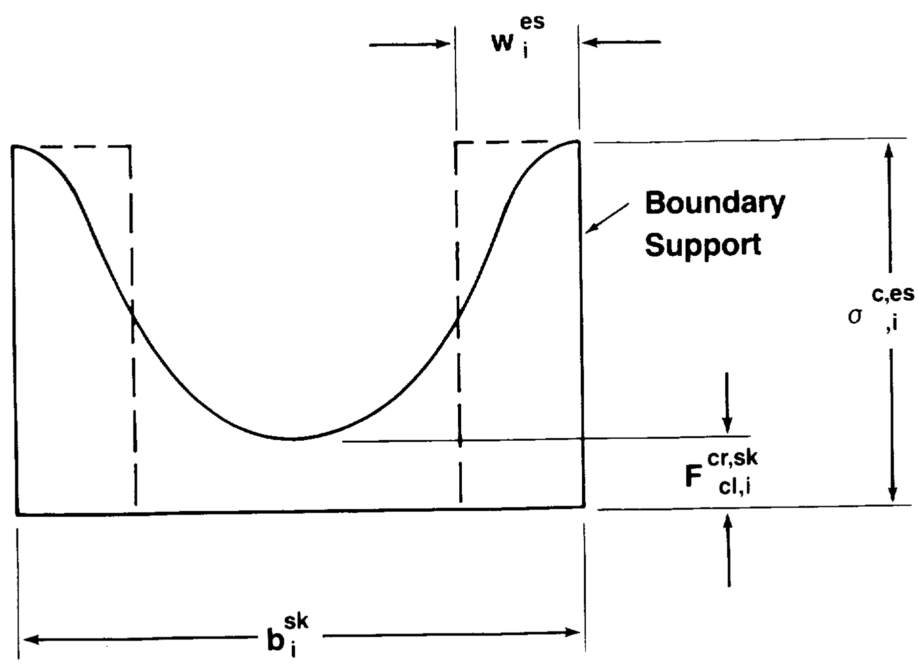

Effective-Width Equation (von Karman):

$$w^{es}_i = (b^{sk}_i/4)[1 + (F^{cr,sk,\Phi E}_{cl,i,f_\chi}/\sigma^{c,es}_{,i})]$$

Middle Stiffener with Skin Effective-Widths

The detail buckling and crippling analysis is directed at this cross section. The calculations focus on only the middle stiffener which carries one-third of the total load up to crippling. The predicted crippling load of the middle stiffener and skin is equal to the summation of the stiffener element pseudo-crippling loads and the effective-width skin load.

$$P_{*,i}^{cc,ses} = [\ Ca(P_{*,i}^{cc,b}) + 2(P_{*,i}^{cc,f} + P_{,i}^{c,es})]$$

$$P_{,i}^{c,es} = (\sigma_{,i}^{c,es})*(\hat{w}_i^{es})*(t_i^{sk}), \quad \text{where} \quad \hat{w}_i^{es} = (w_i^{es} - b_i^f)$$

Pertinent dimensions and effective-widths are shown.

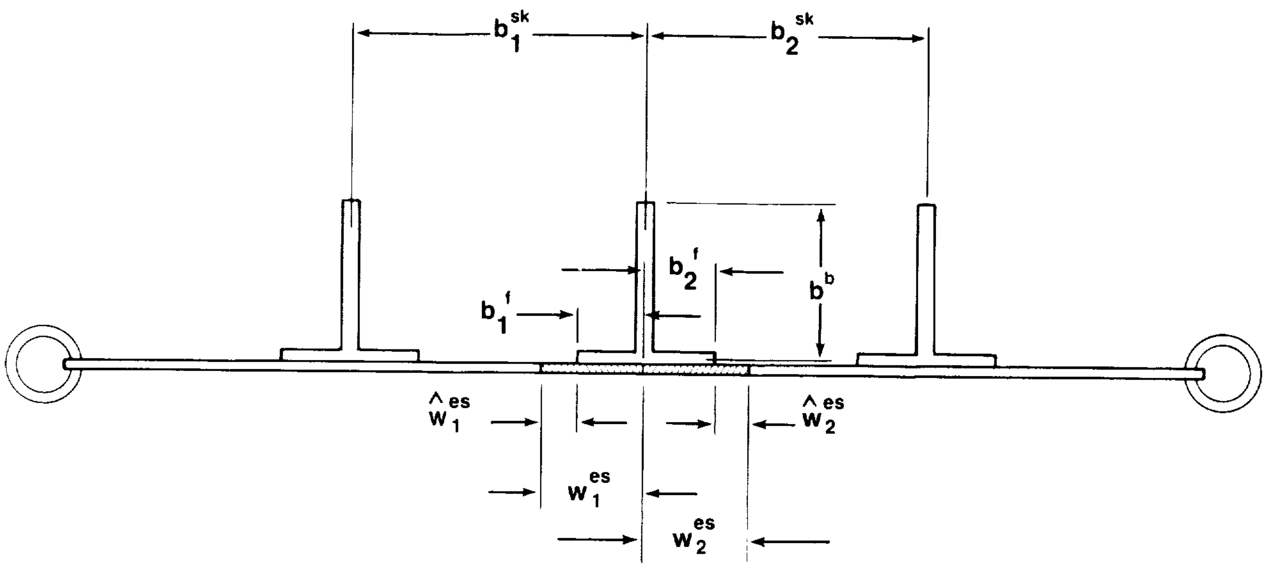

Strain Gage Locations on stiffened Panel

Before the analytical results are presented, an examination of the test data is required. This examination includes a review of strain gauge locations, an investigation of strain results, and finally, photographs of the test panel at different stages of postbuckling.

Twenty-four strain gauges were mounted on the test panel. Only those gauges that were actually used in the evaluation are shown. Test results indicate that compressive strain was uniform up to skin buckling. In addition, buckling of stiffener elements (i.e., blade and flanges) was also detected.

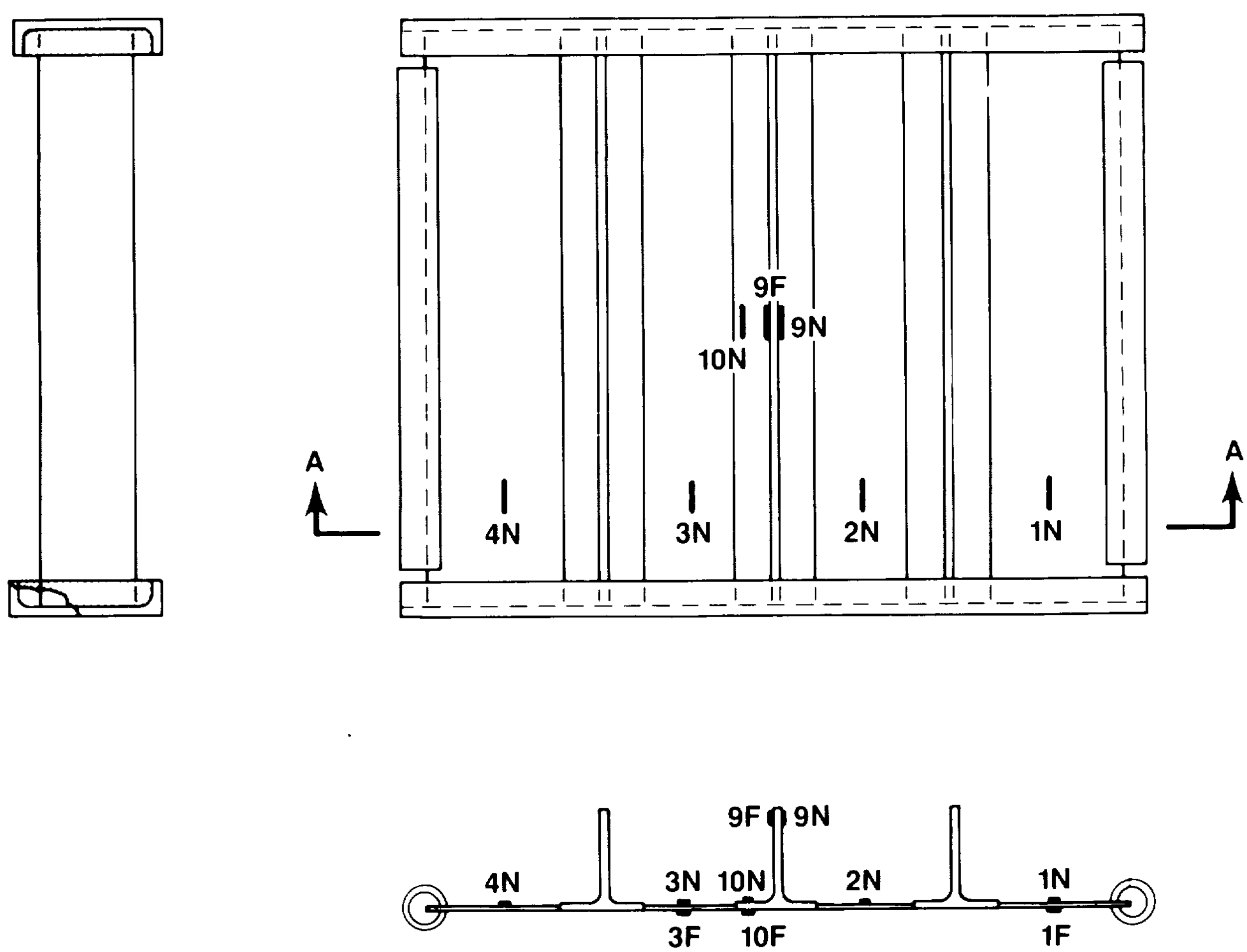

Section A-A

Load/Strain Curves Across Panel

Uniform strain was found in the central panels up to skin buckling as shown by gauges 1N through 4N. Although one of the outer panel gauges (1N) is displaced from the others, it has the same slope. These gauges indicate that the applied compression load was uniform.

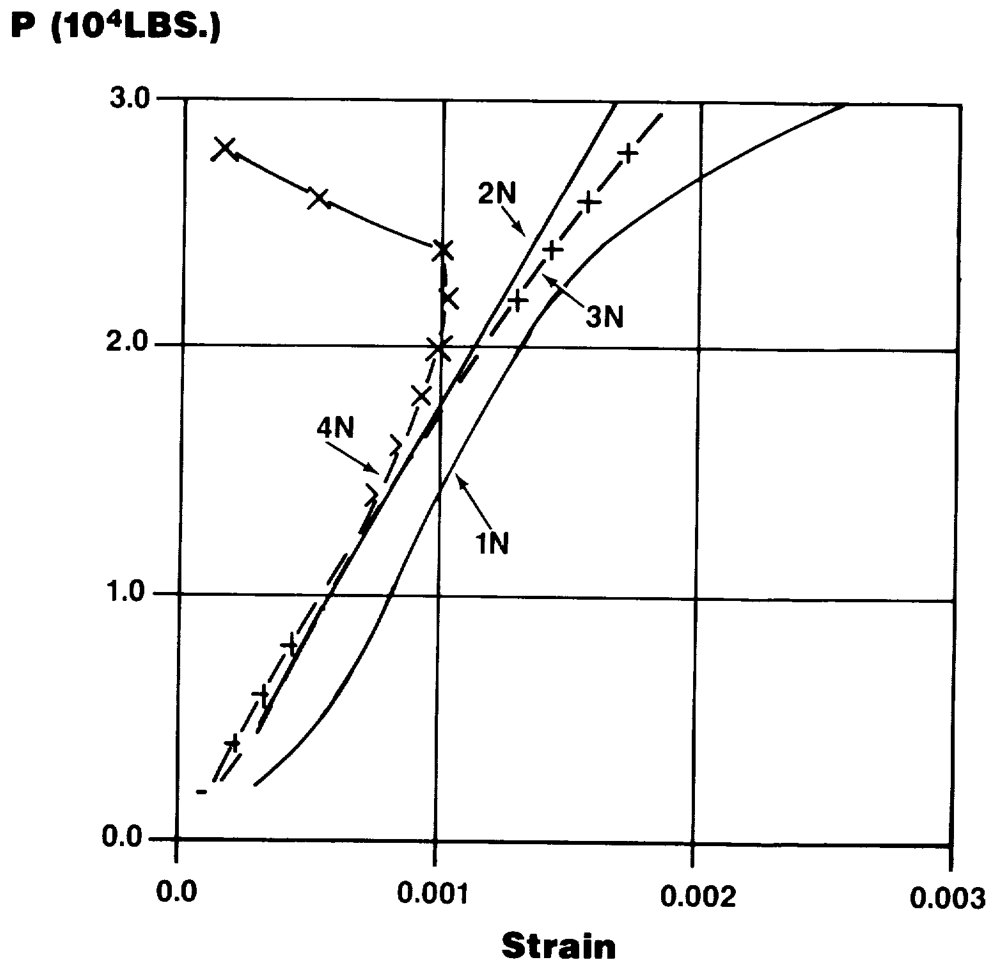

Back-To-Back Load/Strain Plots in Inner Skin Panel

The postbuckling behavior of the inner panels, based upon gauges 3N & 3F, was moderately nonlinear. This plot indicates that buckling occurred between 20,000 Lbs and 25,000 Lbs.

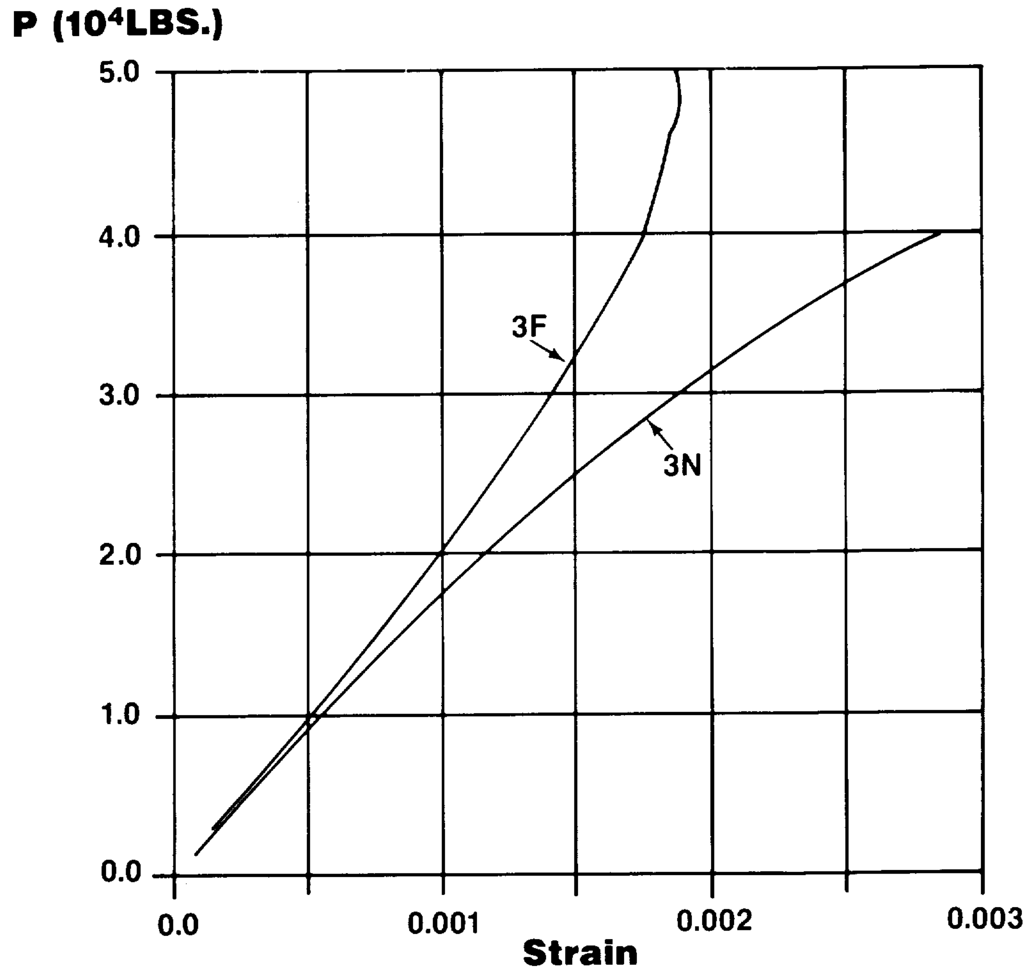

Back-To-Back Load/Strain Plots in Outer Skin Panels

The postbuckling behavior of the outer panels, based upon gauges 1N & 1F, was quite nonlinear. This plot indicates that buckling occurred between 22,000 Lbs and 24,000 Lbs.

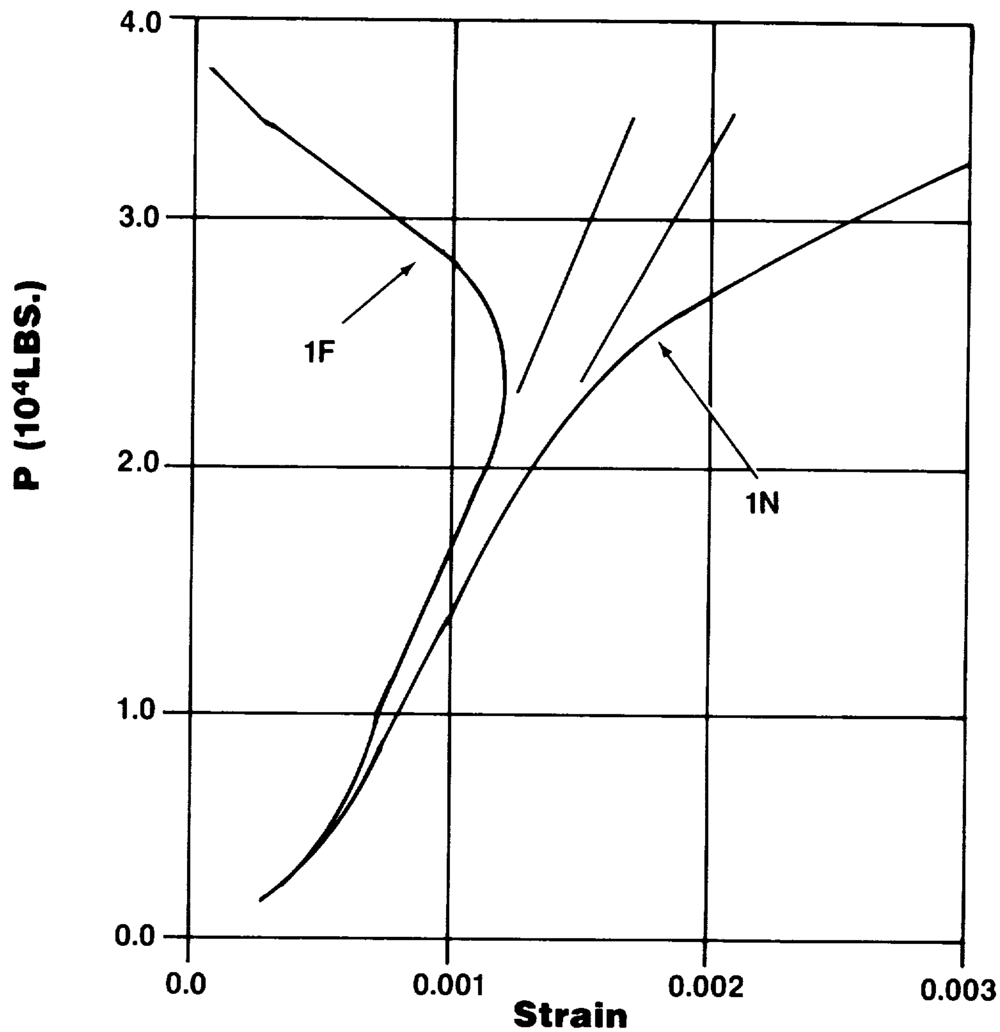

Back-to-Back Load/Strain Plots at Tip of Middle Blade

The lateral buckling of the middle stiffener's blade is indicated by the plot of back-to-back gauges 9N and 9F. Initial buckling appears to occur at a panel load of about 32,000 lbs, where the postbuckling behavior is slight up to a load of about 42,000 lbs. Beyond this load level, significant buckling deformation begins.

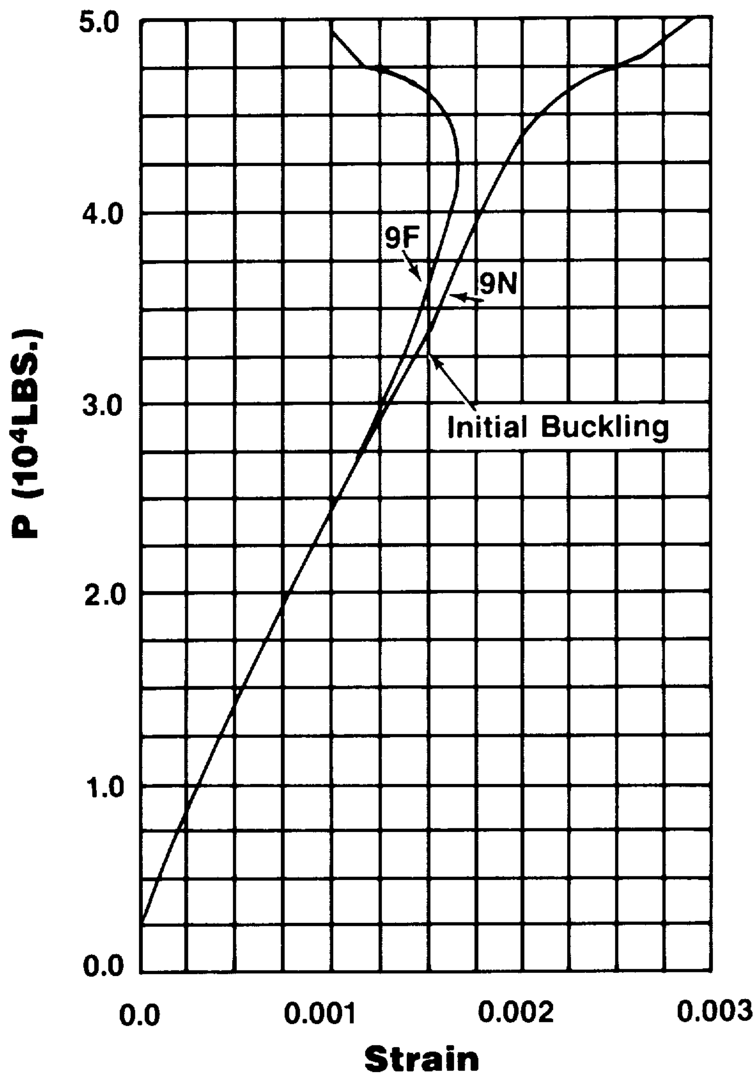

Back-To-Back Load/Strain Plots on Flange of Middle Stiffener

The behavior of one of the stiffener flanges is shown by the back-to-back gauges 10N and 10F. The load-strain plots are nearly linear up to a panel load of approximately 40,000 lbs. Buckling becomes quite evident at a panel load of about 45,000 lbs, which is slightly greater than that previously shown for the blade.

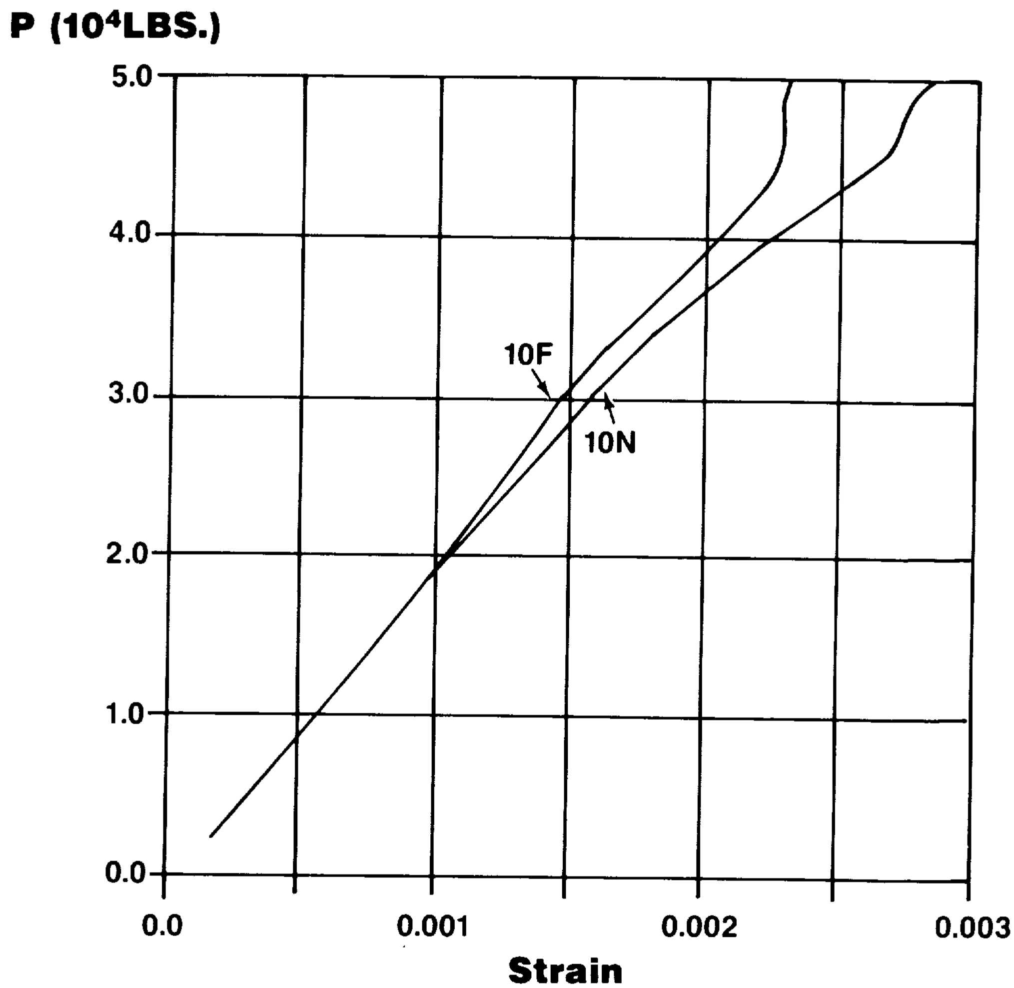

Postbuckling Behavior of Blade-Stiffened Panel at 48,000 Lbs

The compressive load on the stiffened panel is 48,000 lbs. At this load, strain gauges indicate that both the skin and blades have buckled. Note that the split steel tubes have been mounted on the outer unloaded edges.

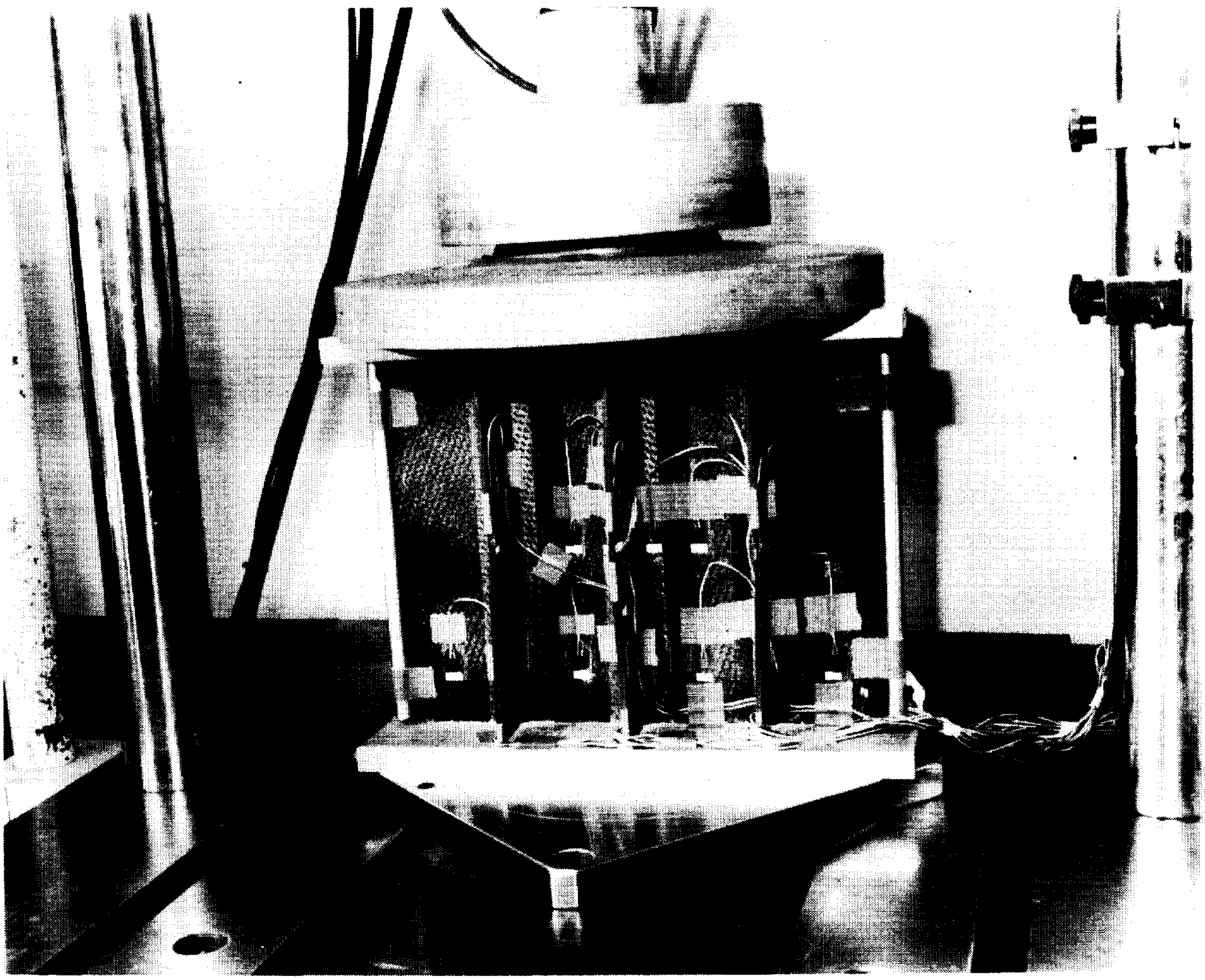

Postbuckling Behavior of Blade-Stiffened Panel at 55,600 Lbs

At 55,600 lbs., the buckling of the skin, and particularly the blades, has become quite severe. However, out of plane deformation will become much greater before crippling occurs.

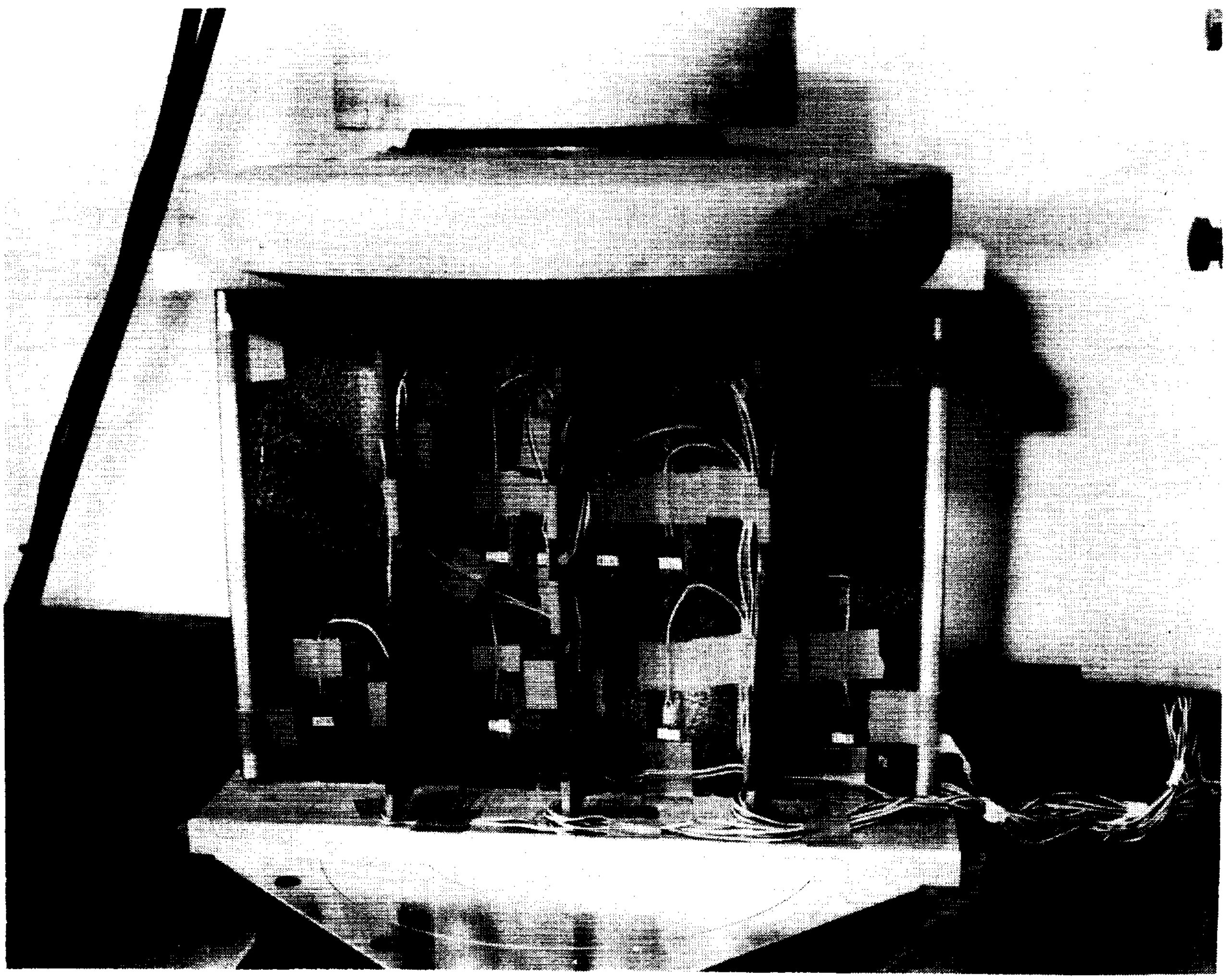

Postbuckling Behavior of Blade-Stiffened Panel at 67,750 Lbs

The crippling load of the stiffened panel was 67,750 pounds. The failed specimen is shown after being removed from the test rig. Note the severe crimping of the skin and the extensive delamination of the left blade. The postbuckling forces of the outer skin panels also severely bent the steel split tubes.

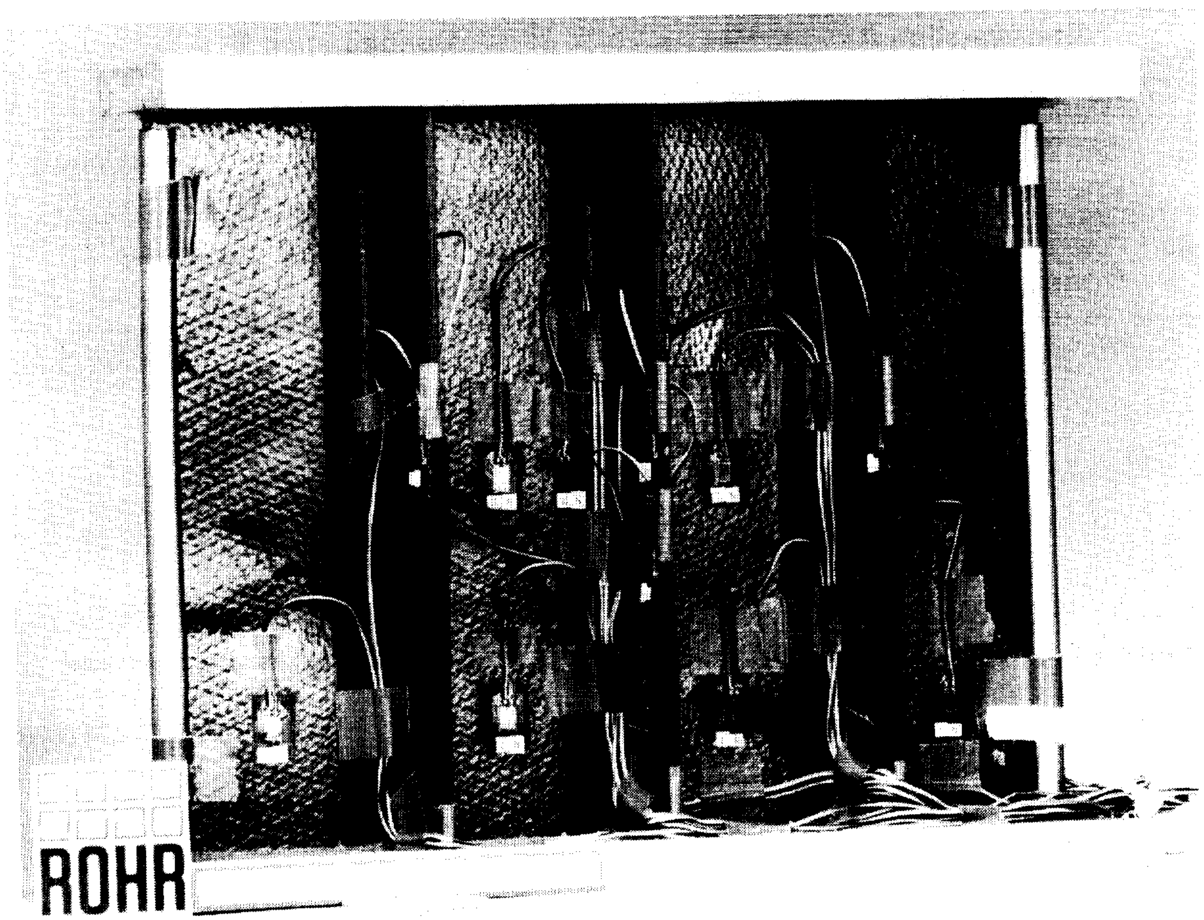

Stability Analysis Boundary Conditions

For completeness, buckling and crippling predictions were obtained for two boundary condition configurations. Configuration A represents simply supported boundary conditions. Configuration B represents boundary restraint between simply supported and fully fixed. The results are presented in the following table.

Configuration A		Configuration B	
Skin	Both Edges Simply Supported	Skin	Both Edges Fixed
Blade	One Edge Simply Supported One Edge Free	Blade	One Edge Simply Supported/Fixed One Edge Free
Flange	One Edge Simply Supported One Edge Free	Flange	One Edge Simply Supported One Edge Free

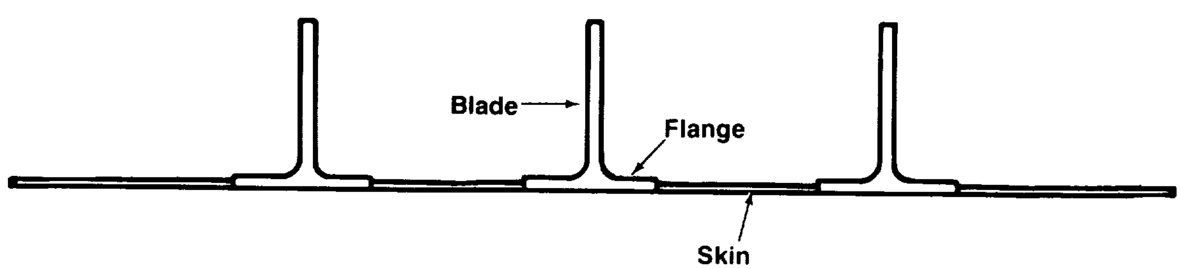

A Comparison of Test and Analysis Results

This table shows the comparisons between test and analysis for the configurations just defined. The analysis is conservative for both configurations. However, Configuration B provides much closer agreement between test and analysis for both buckling and crippling. The predicted buckling strength is about 12% conservative and the predicted crippling load is about 17% conservative.

In conclusion, a test to failure of a blade-stiffened carbon/epoxy stiffened panel has been presented. Axial strain gauges were employed to verify uniformity of axial strain prior to any local buckling. In addition, back-to-back axial strain gauges were used for detection of initial buckling and postbuckling behavior of the skins, blades, and flanges. The stiffened panel behaved as designed. The skins buckled first, the blades second, and the flanges last. In the analysis, it was assumed that crippling of a blade occurred first, where initial failure would be at the supported edge, the location of maximum compressive stress. A videotape of the test was made, and it appeared that failure did indeed start at one of the blade/skin intersections.

	Test Result	Analysis			
		Configuration A		Configuration B	
Stability Mode	Load (Lb.)	Load (Lb.)	Difference (%)	Load (Lb.)	Difference (%)
Buckling	≈23,000	12,600	45	20,200	12
Crippling	67,750	41,000	39	56,300	17

Symbols and Abbreviations

A_i^u	area of element "i", type "u"
b	blade
b/t	width over thickness ratio
b_i^b	Height of blade element "i"
b_i^f	width of flange element "i"
b_i^{sk}	width of skin element "i"
C	end-fixity coefficient of column: approximately equal to 3.6 for potted end columns in a test machine
Ca	correction factor for edge support of blade and stiffener
D_{ij}	flexural/twisting stiffness terms of laminated plate
$E_{Th,i}^{c,u}$	in-plane compression modulus of element "i", type "u"
F^{cc}	crippling stress (psi)
$F_{*,i}^{cc,u}$	expected crippling stress of element "i", type "u"
F^{cr}	buckling stress (psi)
F_{cl}^{cr}	classical buckling stress (psi)
$F_{cl,i}^{cr,sk}$	classical buckling stress of skin element "i"
$F_{*,i}^{cr,u}$	expected buckling stress of element "i", type "u"
$F_{cl,i,ss}^{cr,u,\phi E}$	classical buckling strength of a long plate type "u", element "i" with simply supported unloaded edges

Symbols and Abbreviations

$F^{cr,u,\phi E}_{cl,i,fx}$	classical buckling strength of a long plate type "u", element "i" with fixed unloaded edges
$F^{cr,u,1E}_{cl,i,ss}$	classical buckling strength of a long plate type "u", element "i" with one simply suppported unloaded edge
F^{cu}	ultimate compression strength (psi)
$F^{cu,u}_{n\ ,i}$	ultimate compression strength of element "i", type "u", and data type "n"
i	element number (i.e., each stiffener has 1 blade, 2 flanges and 2 skins)
L	column length
L'	effective column length ($L' = L \div \sqrt{C}$)
n	data type (i.e., empirical "Em", classical "cl", or theoretical)
$P^{c,es}_{\ ,i}$	compression load in effective skin element "i"
P^{cc}	crippling load (lbs)
$P^{cc,b}_{*\ ,i}$	expected crippling load of blade element "i"
$P^{cc,f}_{*\ ,i}$	expected crippling load of flange element "i"
$P^{cc,ses}_{*,i}$	expected crippling load of stiffener/effective skin element "i"
P^{cr}	buckling load (lbs)
t	thickness (inch)
t^{sk}_{i}	thickness of skin element "i"
u	element type (i.e., blade "b", flange "f", stringer "st", skin "sk", effective skin "es", stiffener/skin "sts", stiffener/effective skin "ses", panel "p")

Symbols and Abbreviations

w_i^{es}	effective width of skin element "i"
$\hat{w}_i^{es}$	effective width of skin element "i" excluding the width of the adjacent stiffener flange
$\epsilon_*^{cr,st}$	expected buckling strain of stiffener element "i"
$\sigma_{,i}^{c,es}$	compression stress of effective skin element "i"

REFERENCES

1. Spier, E.E., "Stability of graphite/epoxy Structures with Arbitrary Symmetrical Laminates", "Experimental Mechanics", Vol. 18, No. 11, November 1978, pp 255-271.

2. Spier, E.E., and Klouman, F.L., "Empirical Crippling Analysis of graphite/epoxy Laminated Plates", Composite Materials: Testing and Design (4th Conference), ASTM STP 617, 1977, pp 255-271.

3. Spier, E.E., "On Experimental Versus Theoretical Incipient Buckling of Narrow graphite/epoxy Plates in Compression", AIAA-80-0686-paper, published in "Proceedings of AIAA/ASME/AHS 21st Structures, Structural Dynamics and Materials Conference, May 12-14, 1980, pp 187-193.

4. Spier, E.E., and Klouman, F.L., "Ultimate Compressive Strength and Nonlinear Stress-Strain Curves of graphite/epoxy laminates", Proceedings 8th National SAMPE Conference, "Bicentennial of Materials Progress - Part II", Seattle, Washington, October 1976, pp 213-223.

5. Spier, E.E., and Klouman, F.L., "Postbuckling Behavior of graphite/epoxy Laminated Plates and Channels", Army Symposium on Solid Mechanics, Composite Materials: The Influence of Mechanics of Failure on Design, Cape Cod, Mass., September 1976, pp 62-78.

6. Spier, E.E., "Local Buckling, Postbuckling, and Crippling Behavior of graphite/epoxy Short Thin Walled Compression Member", NASC-N100019-80-c-0174, July 1981.

7. Almroth, B.O., et al, Structural Analysis of Generals Shells, User Instructions for STAGSC, Vol. III, Report No. LMSC D502277, Lockheed Structural Mechanics Laboratory, Lockheed Palo Alto Research Laboratory, Palo Alto, California, December 1975.

8. Arnold, R.R., and Mayers, J., "Buckling, Postbuckling, and Crippling of Materially Nonlinear Laminated Composite Plates", International Journal of Solids and Structures, Vol. 20, No. 9/10, 1984, pp 863-880.

9. von Karman, Th., Sechler, E., and Donnell, L., "The Strength of Thin Plates in Compression", Trans. ASME, Volume 54, Number 2, June 30, 1932.